

# Nanoparticle removal and exhaust gas cleaning using a gas-liquid interfacial nonthermal plasma

Tomoyuki Kuroki <sup>a\*</sup>, Shunsuke Nishii <sup>a</sup>, Takuya Kuwahara <sup>b</sup>, and Masaaki Okubo <sup>a</sup>

<sup>a</sup> Dept. of Mechanical Engineering

Osaka Prefecture University

1-1 Gakuen-cho, Naka-ku, Sakai 599-8531, Japan

<sup>b</sup> Dept. of Products Engineering and Environmental Management

Nippon Institute of Technology

4-1 Gakuendai, Miyashiro-machi, Minamisaitama, Saitama 345-8501, Japan

\* Corresponding author. Tel./fax : +81-72-254-9233

e-mail: kuroki@me.osakafu-u.ac.jp

**Abstract**—The removal of air pollutants containing nanoparticles with a wet-type plasma reactor is investigated by using a gas-liquid interfacial nonthermal plasma. This reactor can simultaneously remove nanoparticles and harmful gases such as nitrogen oxides ( $\text{NO}_x$ ) and sulfur oxides ( $\text{SO}_x$ ). In order to evaluate the performance of this reactor, a simulated exhaust gas is prepared using polystyrene latex particles having diameters of 29, 48, 100, 202, and 309 nm, and  $\text{NO} / \text{SO}_2$  gas cylinders. A collection efficiency of more than 99% is achieved for nanoparticles having diameters in the 27.9–216.7 nm range. Moreover, removal efficiencies of more than 99% and 77% are obtained for  $\text{SO}_2$  and  $\text{NO}_x$ , respectively. From these results, it is confirmed that this wet-type pulsed corona discharge plasma reactor is useful for the simultaneous removal of nanoparticles,  $\text{NO}_x$ , and  $\text{SO}_x$ .

**Keywords:** Air cleaner, nonthermal plasma, electrostatic precipitator, gas-liquid interface, nanoparticle,  $\text{NO}_x$ ,  $\text{SO}_x$ .

## I. INTRODUCTION

Particulate matter (PM), nitrogen oxides ( $\text{NO}_x = \text{NO} + \text{NO}_2$ ), and sulfur oxide ( $\text{SO}_x = \text{SO}_2 + \text{SO}_3$ ) emitted from diesel engines, thermal power generation plants, and general factories of industries have bad effect for global environment and humans. Therefore, they become a great problem, and nonthermal plasma technology is one of the important treatment method attracting attentions [1–7]. Especially, in Asia region, recently, suspended nano-sized particles in the atmosphere among the harmful air pollutants have become an international problem.  $\text{PM}_{2.5}$  represents the particle having an aerodynamic diameter less than 2.5  $\mu\text{m}$ .

Especially, smaller particles or nanoparticles having an aerodynamic diameter of approximately 100 nm are very harmful for health and induces respiratory diseases because they easily deposit and proceed to the inner cells in the respiratory tube and lung wall.

Under these circumstances, various kinds of researches on indoor air cleaner the target of which is the removal of  $PM_{2.5}$  in the world, especially Asian countries. On the other hand, in the accident of the nuclear power plants in Japan in 2011, radioactive gaseous or particulate air pollutants are temporarily released from the nuclear reactors and their removals were required. Generally, particulate matter suspended in the atmosphere can be collected by the air cleaner where polymer filters (HEPA or ULPA filters) combined with fan apparatus. These types of air cleaner were used in the nuclear power plant after the accidents occur. However, in the case with air cleaner with the filters radioactive matters inside the filters during filtering become a problem should be treated properly. Furthermore, it is difficult to achieve high-efficient removals of gaseous molecules air pollutants are difficult with polymer filters, and increased pressure loss with the deposition of particles in the filter induces the energy loss in the fan. On the other hand, most small indoor air cleaners for industries and home use developed and purchased in the market are air-filter type. Therefore, for the removals of gaseous harmful radioactive air pollutants such as radioactive iodine, I 131 and cesium, Cs 137 which were emitted from the nuclear power plant during the accident and suspended in the atmosphere, and suspended nanoparticle connected with these harmful matter, a compact air-cleaner which does not use the filters should be newly developed and it is very meaningful.

Under these backgrounds for the present research, we propose a system where a wet-type electrostatic precipitator [8, 9] is combined with an atmospheric-pressure nonthermal plasma (NTP) generator for the removal of nanoparticle pollutants suspended in the atmospheric environment. As used in our previous papers [10–12], we named this system “wet-type plasma reactor”. In the wet-type plasma reactor, there are merits that the decrease in the collection efficiency due to the re-entrainment observed in dry electrostatics precipitator does not occur, and high collection efficiency for nano meter sized particles is achieved. In the apparatus, pulsed high-voltage is applied between the electrodes and positive ions are induced. As a result, particulate matter in the channel is charged and collected inside the water film on the grounded electrode. After the collection, pollutants are cleaned with high efficiency by treating the waste water.

In the present report, as a basic study for this type of actual-scale system, experimental model and principle of chemical reactions for nanoparticle collection performances of wet-type plasma reactor are described with experimental results. Furthermore, not only PM, but also  $NO_x$  and  $SO_x$  simultaneous removal which emits from factories is carried out using aqueous solution using reducing chemical agents [10, 11].

## II. EXPERIMENTAL APPARATUS AND PRINCIPLE OF CLEANING REACTIONS

### A. Experimental apparatus

**Figure 1** shows schematics of the wet-type plasma reactor used in the experiment. In the research, this type of apparatus where electrostatic precipitator for particulate removal are combined with wet-chemical reactor for solution scrubbing. This system is superior to the ordinary air cleaner because the polymer filter is not used. This reactor is a laboratory-scale

model with cylindrical channel of 20 mm and length of the grounded electrode of 260 mm. This apparatus consists of a pair of discharge electrodes and water film on the wall in the channel. The air pollutants are introduced to the channel and cleaned up. By applying the pulsed high-voltage between the electrodes ions are induced to charge the particulate matter flowing in the channel. As a result, PM is collected inside the water film near the grounded electrode. More than 95% of nanoparticles can be collected and it is superior performance. On the other hand, gaseous air pollutants flowing in the channel is treated by the NTP. Further, electrostatic wind induced by the moving ions stirs the flow to absorb into the aqueous solution film. Waste water solution should be treated and vaporized, condensed, and treated in the case of radioactive particle chemically and finally becomes solid. However, for low-level harmful pollutant, it can be drained to sewage as it is. As an aqueous solution, the following reducing agents are suitable for  $\text{NO}_x$  and  $\text{SO}_x$  simultaneous removal.

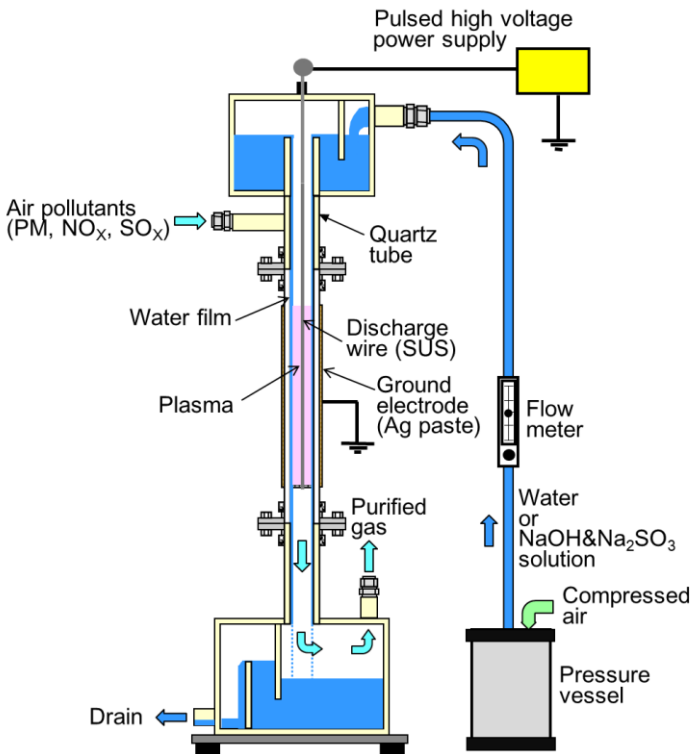


Fig. 1. Schematics of wet-type plasma reactor

### B. Principle of cleaning reactions

A mechanism and principle of simultaneous removal of PM, NO<sub>x</sub>, and SO<sub>x</sub> in the system is described. As an aqueous solution, NaOH solution, Na<sub>2</sub>SO<sub>3</sub> solution and their mixtures are used [10–16]. NO gaseous component passing through the wet-type reactor reacts with N<sub>2</sub> and O<sub>2</sub> in the and partially reduce to nitrogen, but mostly oxidized air by the NTP to NO<sub>2</sub>.



where  $\bullet\text{N}$  and  $\bullet\text{O}$  means nitrogen and oxygen radicals,  $e$  denotes electron, and  $\text{M}$  represents third materials (N<sub>2</sub> and O<sub>2</sub>). The reaction (3) progresses by NTP under the existence of oxygen radical  $\bullet\text{O}$ . NO<sub>2</sub> obtained by the oxidation reaction (3) is water-soluble and removed by the reaction on Na<sub>2</sub>SO<sub>3</sub> aqueous solution, the NO<sub>2</sub> is converted and reduced to N<sub>2</sub> and non-toxic water soluble Na<sub>2</sub>SO<sub>3</sub> according to the chemical reaction.



When the aqueous solution is NaOH, Na<sub>2</sub>SO<sub>3</sub> is generated according to the chemical reaction (5) between SO<sub>2</sub> included in the exhaust and NaOH to remove SO<sub>2</sub> and enhance the reducing reaction (3) for NO<sub>2</sub>



On the other hand, SO<sub>2</sub>, SO<sub>3</sub>, and NO<sub>2</sub> are water-soluble and as a result, H<sub>2</sub>SO<sub>4</sub>, HSO<sub>3</sub>, HNO<sub>2</sub>, and HNO<sub>3</sub> are induced in the solution.



The pH in the solution decreases as reaction (6) – (8) progresses. However, NaOH added in the solution contributes the neutralization. On the other hand, when pH of the aqueous solution is more than eight or strong alkaline solution, carbon dioxide (CO<sub>2</sub>) is also absorbed to the solution film. Generally, because CO<sub>2</sub> concentration in the exhaust gas is high, in % order the solution becomes slightly acid. However, when NaOH is added to the solution, Potassium hydrogen carbon trioxides NaHCO<sub>3</sub> and Na<sub>2</sub>CO<sub>3</sub> are generated and the solution becomes pH buffer one to keep it slightly alkaline. Furthermore, it is known that denitration based on the reaction (4) is effective for alkali solution of pH ~ 8.

It is known from these explanations that simultaneous removal of NO<sub>x</sub> and SO<sub>x</sub> based on the reactions (1) – (8) is highly consistent technique. Next, some laboratory-scale experimental results on PM, NO<sub>x</sub>, and SO<sub>x</sub> simultaneous removal are reported based on the principle and the experimental model.

### III. EXPERIMENTAL APPARATUS AND METHOD

**Figure 2** shows a layout of the experimental apparatus. Cylinders of synthesized air and gaseous cylinders ( $N_2$  : 79% +  $O_2$  : 21%) are prepared. Aerosol flows of polystyrene latex nanoparticle are generated by passing the air through the spray-type aerosol generator (Model 3076, TSI Co.). The flow rate of the air is controlled by a mass flow controller (SFC280E, Hitachi Metal Co.). Generated aerosol flow passes through the gaseous dryer and becomes in charge equilibrium state using an americium neutralizer. The whole aerosol becomes electrically neutral. The gas including the particles is mixed with the bypassed air flow for dilution, and introduced to the wet-type plasma reactor. As already shown in **Fig. 1**, the plasma reactor has an overflow reservoir of aqueous solution upper region of it. The solution overflowed from this reservoir flows on the inner surface of the reactor to generate the solution film the thickness of which is typically 0.5 mm. As a high voltage power supply, IGBT (Insulated Gate Bipolar Transistor) driven a pulsed high voltage power supply (PPCP Pulsar, SMC-30/1000, 500 W, Masuda Research Inc.) is used. The NTP is induced between the discharge wire and the grounded electrode which is located on the outside surface of insulated (quartz) tube made with liquid silver paste, by applying the high voltage pulse (half value width  $\sim$  400 ns) between the electrode. The applied voltage, current, and instantaneous power waveforms are measured with a digital oscilloscope (DL1740, Yokogawa Electric) through the voltage probe (P6015A, Sony Tektronix) and the current probe (P6021, Sony Tektronix). In order to evaluate the collection efficiency for each particle diameter or the partial collection efficiency of the wet-type plasma reactor, SMPS (scanning mobility particle sizer, CPC Model 3776 + DMA Model 3081, TSI Inc.) is used for measuring the partial collection efficiency before and after the treatment. For the experiment of  $NO_x$  and  $SO_x$  simultaneous removal. the concentrations of  $NO_x$  and  $SO_x$  are adjusted to  $NO = 200$  ppm and  $SO_x = 200$  ppm at the inlet of the plasma reactor. During the wet-type plasma reactor is working and simultaneous removal of  $NO_x$  and  $SO_x$  is carried out, the removal efficiencies of various gaseous components and byproducts are measured and evaluated.  $NO_x$  is measured by a  $NO_x$  analyzer (PG-240, Chemiluminacense, Horiba Ltd.),  $N_2O$  is measured by a  $N_2O$  analyzer (VIA-510, Horiba Ltd.), and  $SO_2$   $H_2SO_4$ ,  $HNO_3$ , and ozone are measured using gas detection tubes (Gastec Co.). During the plasma is turned on, ozone is induced and damages the measurement apparatus, especially, rubber parts. Therefore, an electrical tubular type heater (KRO-14K, Isuzu Co.) is put on the upstream of the measuring apparatus. The temperature is set at  $250^\circ C$  to increase the exhaust gas temperature and remove ozone.

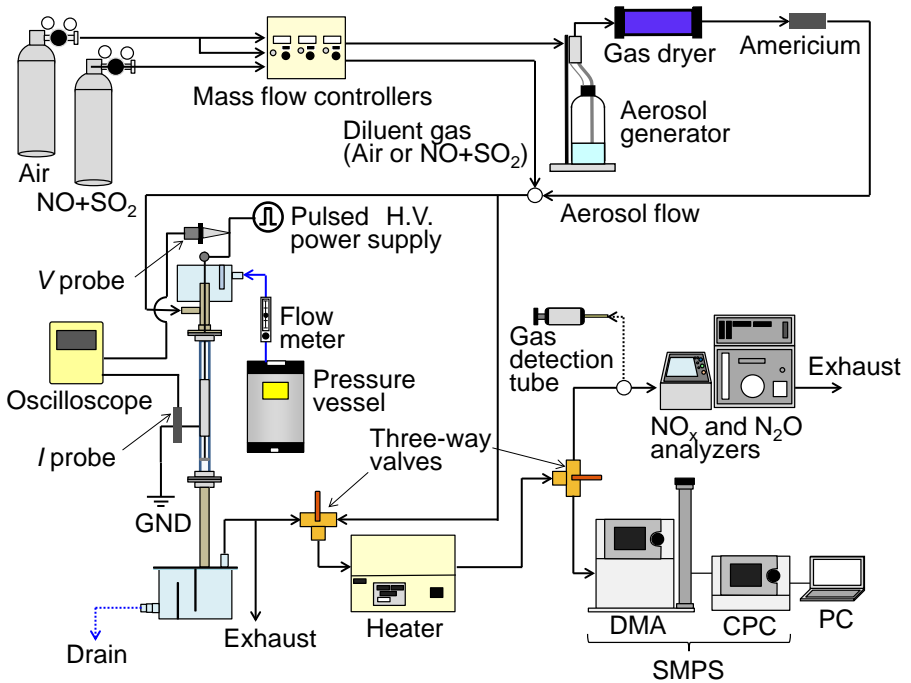


Fig. 2. Experimental setup for simultaneous removal of nanoparticle,  $\text{NO}_x$ , and  $\text{SO}_2$

#### IV. EXPERIMENTAL RESULTS AND DISCUSSION

##### A. Electrostatic precipitation for nanoparticle removal

Figure 3 shows an example of measured voltage, current, and power waveforms. The plasma power is calculated by integrating the  $VI$  over a period with time. The power is used for both electrostatic precipitation and gaseous components decomposition. Figure 4 shows the measurement results on the collection efficiency for a total flow rate of 4 L/min and the grounded electrode length of 260 mm with different solution flow rates of 100 mL/min. In the figure, when the applied voltage is greater than 26 kV, more than 99 % particles are collected in the range of the particle diameter of 15 ~ 414 nm. For the solution flow rate of 50 mL/min, similar result to that of Fig. 4 is obtained. However, for the smaller solution flow rate of 25 mL/min, the collection efficiency obviously decreases overall range of particle size. This is caused by the unstable solution film due to the decrease in the solution flow rate. Especially, the collection efficiency decreases greatly in the diameter ranges of 15 ~ 40 nm and 100 ~ 200 nm because the particle concentration in the range is approximately one-tenth than that in the range of 40 ~ 100 nm and the effect of the removal number on the removal efficiency becomes larger.

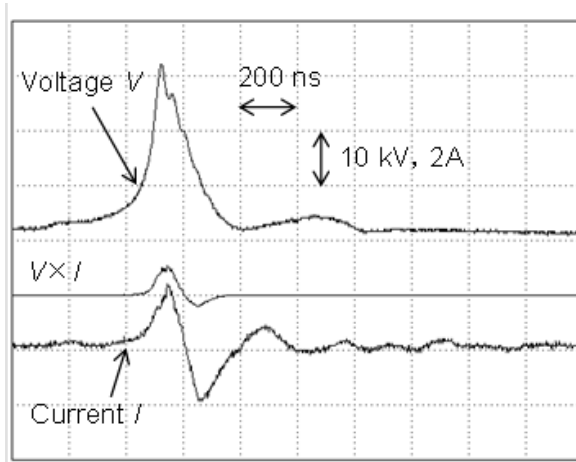


Fig. 3. Voltage, current, and instantaneous power waveforms.

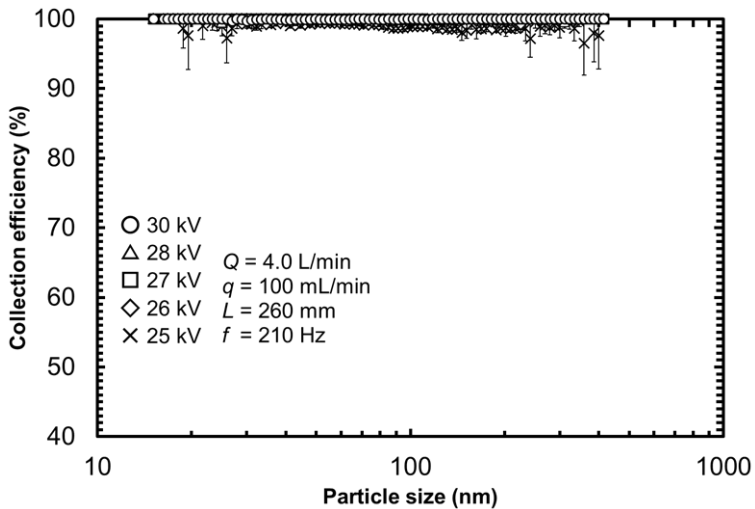
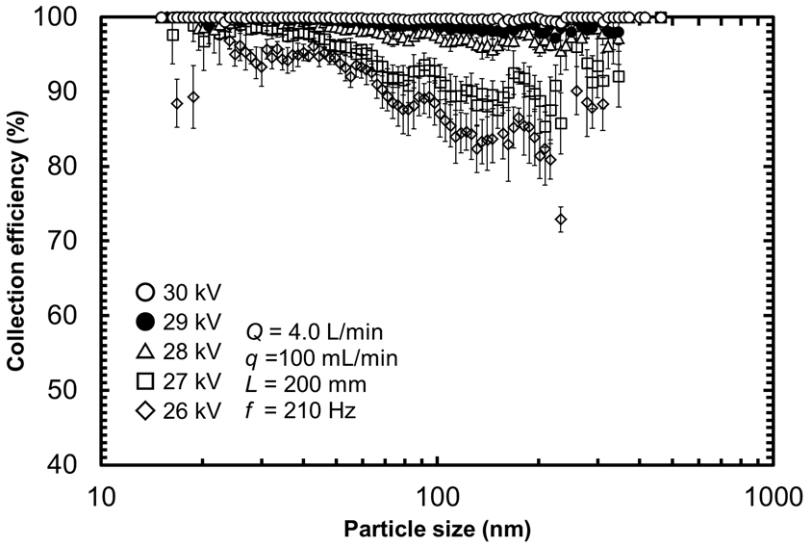


Fig. 4. Effect of solution flow rate on nanoparticle collection efficiency (gaseous flow rate = 4 L/min and the ground electrode length = 260 mm, pulse frequency = 210 Hz, solution flow rate = 100 mL/min, and  $d_p = 15.1 \sim 414.2$  nm).

Next, the length of the grounded electrode is changed to 200 mm, while the other conditions are the same as those in Fig. 4. The result is shown in Fig. 5. It is known from the figure that the collection efficiency reaches more than 99% for all range of the particle diameter only at the applied voltage of 30 kV, and it decreases at lower applied voltage for

the larger diameter range. Especially, at the applied voltage of 26 kV it decreased down to 80% near the diameter of 200 nm. This may be caused by the following reasons: The residence time of the gas at the reactor decreased from 1.2 s to 0.94 s with decrease in the length of the reactor. The particle charging efficiency decreases with decrease in the applied voltage, and the settling velocity of the particles decreases as a result. Furthermore, it is known [17] that the settling velocity becomes in minimum at the submicron range of the diameter near 200 nm.



**Fig. 5.** Nanoparticle collection efficiency for the ground electrode length of 200 mm (the total flow rate = 4 L/min, the solution flow rate = 100 mL/min, pulse frequency = 210 Hz, and  $d_p = 15.1 \sim 461.4$  nm).

Next, the result is shown in **Fig. 6** on the same condition as those in **Fig. 4** except for the increased gas flow rate of 8 L/min. The collection efficiency is almost higher than 99%. However, for 25 kV, it decreases down to 74% for the particle diameter near 200 nm.

Next, the voltage is fixed at 30 kV and the frequency of the pulse high voltage is changed from 10 ~ 210 Hz. The result is shown in **Fig. 7** when the gas flow rate is set at 4 L/min. More than 99% of removal efficiency can be kept when the frequency is decreased down to 50 Hz. It is known from the result that the operation at 105 Hz can be reduced energy by 50% than that at 210 Hz because the power consumption is proportional to the frequency. Next, for the gas flow rate of 8 L/min, and the applied voltage of 30 kV, more than 99% collect on efficiency is achieved when the frequency is equal to or more than 105 Hz. However, for the frequency is equal to or less than 50 Hz, it decreases, for example, it decreases down to 96% for the frequency of 30 Hz and at the particle diameter of 195 nm.

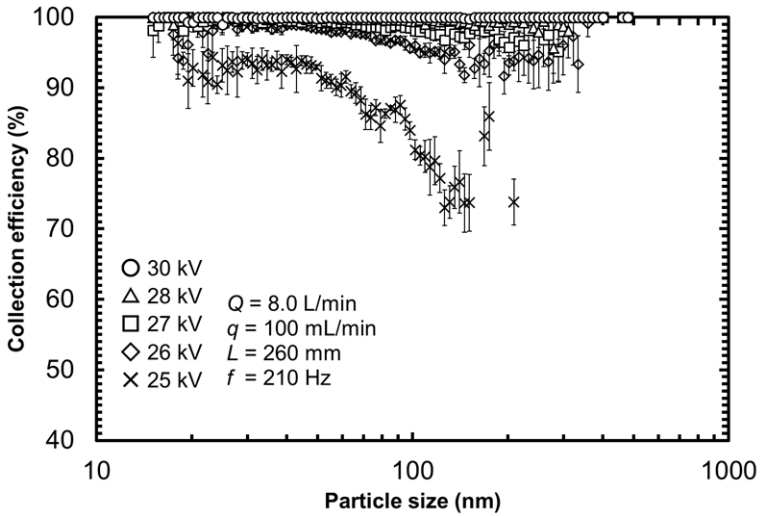


**Fig. 6.** Effect of total gaseous flow rate on nanoparticle collection efficiency (gaseous flow rate = 8 L/min, the ground electrode length = 260 mm, the solution flow rate = 100 mL/min, pulse frequency = 210 Hz, and  $d_p = 15.1 \sim 478.3$  nm).

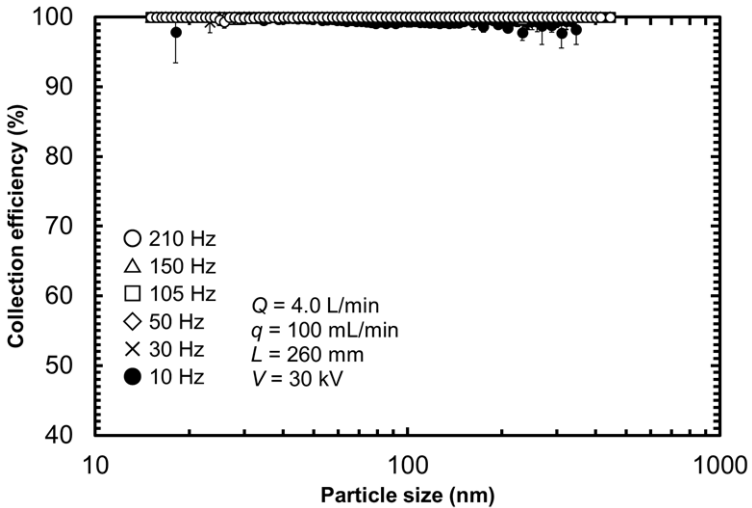


**Fig. 7.** Effect of pulse frequency on nanoparticle collection efficiency (gaseous flow rate = 4 L/min, the ground electrode length = 260 mm, the solution flow rate = 100 mL/min, applied voltage = 30 kV, and  $d_p = 15.1 \sim 478.3$  nm).

**Figure 8** shows the relation between collection efficiency for 101.8 nm particle and the discharge power for different operational conditions. It is known from the figure that for more than 99% collection efficiency the power becomes lowest for the conditions of  $L = 260$  mm,  $f = 105$  Hz, and  $V = 26$  kV.

Based on the experimental results on particles above, further experiment on simultaneous removal of  $\text{NO}_x$ ,  $\text{SO}_x$ , and PM are carried out. Main experimental results are reported in the next section.

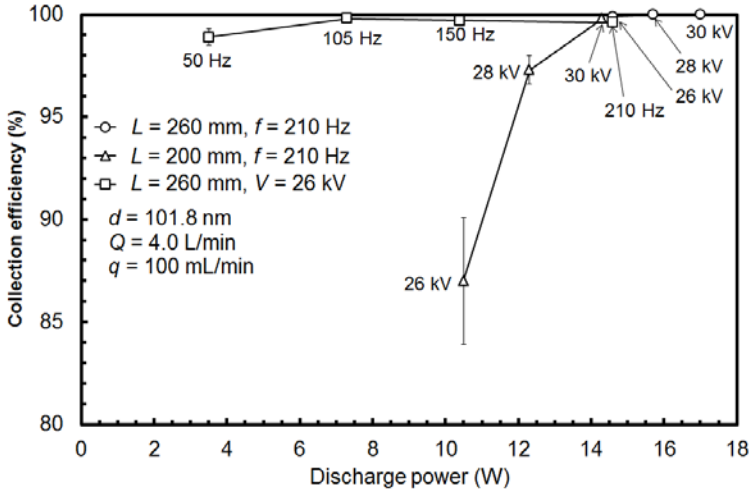


**Fig. 8.** Evaluation of collection efficiency for 101.8 nm particle

### B. Experiment on the simultaneous removal of $\text{NO}_x$ , $\text{SO}_x$ , and PM

**Figure 9** shows an experimental result for the conditions of  $L = 260$  mm and  $f = 105$  Hz when the reducing agent solution of 95 mg/L  $\text{Na}_2\text{SO}_3$  + 30 mg/L NaOH is used as a solution film on the inner wall of the reactor [8].  $\text{NO}_x$  is reduced by the plasma reaction; however, the concentration only decreases down to 87 ppm at the applied voltage of 30 kV. Because  $\text{SO}_2$  is water-soluble, the concentration of  $\text{SO}_2$  decreases down to 2 ppm with the solution flow only, not applying the plasma. The  $\text{SO}_2$  removal efficiency is 99%. It is very effective to use the reducing agent solution.

**Figure 10** shows the results of  $\text{NO}_x$  concentration when the pulse frequency is set at 210 Hz and the concentration of  $\text{Na}_2\text{SO}_3$  increases up to ten-times higher. By increasing the pulse frequency,  $\text{NO}_x$  is reduced by the plasma reaction and the concentration decreases down to 46 ppm at the applied voltage of 30 kV and the  $\text{NO}_x$  removal efficiency of 77% is obtained. With increased  $\text{Na}_2\text{SO}_3$  concentration in the solution, the electrical conductivity is increased. As a result, it is difficult to increase the voltage up to more than 28 kV. When the peak voltage is 28 kV (power = 24 W),  $\text{NO}_x$  concentration is decreased down to 39 ppm.

The removal efficiency is 82% which is slightly increased compared with the case with lower  $\text{Na}_2\text{SO}_3$  concentration.

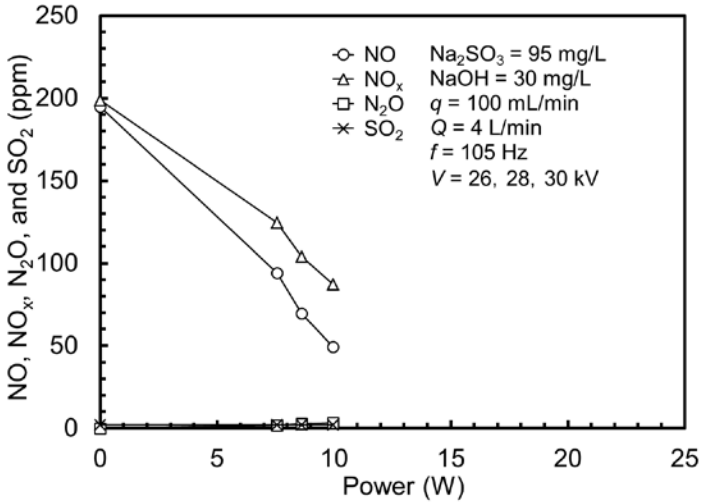


Fig. 9. Simultaneous removal of  $\text{NO}_x$  and  $\text{SO}_x$  under coexisting with nanoparticle for the pulse frequency of 105 Hz (total flow rate = 4 L/min, the ground electrode length = 260 mm).

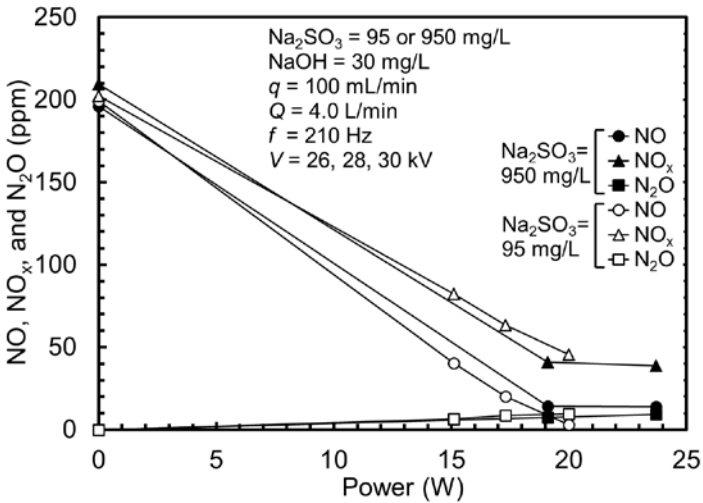


Fig. 10. Effect of  $\text{Na}_2\text{SO}_3$  concentration on  $\text{NO}_x$  removal for the pulse frequency of 210 Hz (total flow rate = 4 L/min, the ground electrode length = 260 mm).

## V. CONCLUSION

A new-type wet type plasma reactor and laboratory-scale model experiment is carried out on the simultaneous removal of PM, NO<sub>x</sub>, and SO<sub>x</sub> using the reactor. In the experiment, 99% of the particles are collected at the applied voltage of 26 kV when the length of the electrode is 260 mm. when the length of the electrode is 200 mm, the collection efficiency decreases down to 80% at the particle diameter of 200 nm. Further, in the test of simultaneous removal of NO<sub>x</sub>, SO<sub>x</sub>, and PM, 77% of NO<sub>x</sub> and 99% of SO<sub>2</sub> removals are obtained on the condition that the exhaust gas flow rate of 4 L/min, initial NO<sub>x</sub> and SO<sub>x</sub> concentrations of 200 ppm, and NTP power of 20 W. In these results, simultaneous removal of NO<sub>x</sub>, SO<sub>x</sub>, and PM is achieved. Based on this fundamental result, farther study toward the development of the actual-scale system for industries will be carried out in the future research.

## ACKNOWLEDGEMENT

The authors greatly thank Mr. K. Iwashiro and Mr. T. Izumi (formally students of Osaka Prefecture University) for their technical support in the experiments. This work is partially supported by TEPCO Memorial Research Grant (General Research).

## REFERENCES

- [1] M. Okubo, Air and water pollution control technologies using atmospheric pressure low-temperature plasma, *J. Plasma Fusion Res.* 84 (2) (2008) 121–134 (in Japanese).
- [2] M. Okubo, H. Fujishima, K. Otsuka, Plasma hybrid clean technology for flue gas emitted from combustors, *J. Plasma Fusion Res.* 89 (3) (2013) 152–157 (in Japanese).
- [3] G. Dinelli, L. Civitano, and M. Rea, Industrial experiments on pulsed corona simultaneous removal of NO<sub>x</sub> and SO<sub>2</sub> from flue gas. *IEEE Trans. Ind. Appl.* 26 (3) (1990) 535–541.
- [4] J. Jolibois, K. Takashima, and A. Mizuno, Application of a non-thermal surface plasma discharge in wet condition for gas exhaust treatment: NO<sub>x</sub> removal, *J. Electrostat.* 70 (2012) 300–308.
- [5] Y. Yoshioka, H. Kondo, Y. Tabata, H. Hatakenaka, and K. Nakada, Automatic control method of NO removal by a combination of ozone injection and exhaust gas recirculation, *IEEE Trans. Ind. Appl.* 46 (3) (2010) 1166–1174.
- [6] S. Kambara, Y. Kumano, and K. Yukimura, DeNO<sub>x</sub> characteristics using two staged radical injection techniques, *IEEE Trans. Diel. and Electr. Insul.* 16 (3) (2009) 778–784.
- [7] M. B. Chang, H. M. Lee, F. Wu, and C. Lai, Simultaneous removal of nitrogen oxide/nitrogen dioxide/sulfur dioxide from gas streams by combined plasma scrubbing technology, *J. Air Waste Manage Assoc.* 54 (2004) 941–949.
- [8] Y. Ueda, Newly Trial to improve performance of wet type ESP, *J. Inst. Electrostat. Jpn.*, 26 (6) (2002) 268–269 (in Japanese).
- [9] H. J. Kim, B. Han, Y. J. Kim, K. D. Hwang, W. S. Oh, S. Y. Yoo, and T. Oda, Fine particle removal performance of a two-stage wet electrostatic precipitator using a nonmetallic pre-charger, *J. Air Waste Management Assoc.* 61 (2011) 1334–1343.
- [10] T. Kuroki, M. Takahashi, M. Okubo, and T. Yamamoto, Single-stage plasma-chemical process for particulates, NO<sub>x</sub>, and SO<sub>x</sub> simultaneous removal, *IEEE Trans. Ind. Appl.* 38 (5) (2002) 1204–1209.
- [11] T. Kuwahara, T. Kuroki, T. Yamamoto, and M. Okubo, Single-stage simultaneous removal of gases and particulates in wet-type plasma-chemical reactor, *Proc. Inter. Symp. Electrohydrodynamics 2012* (2012) 108–113.
- [12] T. Kuroki, S. Nishii, and M. Okubo, Fundamental study on the simultaneous removal of nanoparticle and harmful gas components using a wet-type discharge plasma reactor, *Earozoru Kenkyu* 30 (2) (2015) 108–113 (in Japanese).

- [13] T. Yamamoto, M. Okubo., K. Hayakawa, and K. Kitaura, Towards ideal NO<sub>x</sub> control technology using a plasma-chemical hybrid process, *IEEE Trans. Ind. Appl.* 37 (5) (2001) 1492–1498.
- [14] T. Yamamoto, M. Okubo, T. Nagaoka, and K. Hayakawa, Simultaneous removal of NO<sub>x</sub>, SO<sub>x</sub>, and CO<sub>2</sub> at elevated temperature using a plasma-chemical hybrid process, *IEEE Trans. Ind. Appl.*, 38, 5 (2002) 1168–1173.
- [15] T. Yamamoto, C. L. Yang, M. Beltran, and Z. Kravets, Plasma-assisted chemical processes for NO<sub>x</sub> control, *IEEE Trans. Ind. Appl.* 36 (3) (2000) 923–927.
- [16] C. L. Yang, T. Yamamoto, M. Beltran, and Z. Kravets, Corona-induced chemical scrubber for the NO<sub>x</sub> emission, *Environ. Prog.* 17 (3) (1998) 183–189.
- [17] H. J. Kim, B. Han, Y. J. Kim, S. J. Yoa, Characteristics of an electrostatic precipitator for submicron particles using non-metallic electrodes and collection plates, *J. Aerosol Sci.* 41 (2010) 987–997.